

Dethinning Extensive Air Shower Simulations

B.T. Stokes^{a,*}, R. Cady^a, D. Ivanov^{a,b}, J. N. Matthews^a, G. B. Thomson^a

^aUniversity of Utah, Department of Physics & Astronomy and High Energy Astrophysics Institute, Salt Lake City, Utah 84112, USA

^bRutgers—The State University of New Jersey, Department of Physics and Astronomy, Piscataway, New Jersey 08854, USA

Abstract

We describe a method for restoring information lost during statistical thinning in extensive air shower simulations. By converting weighted particles from thinned simulations to swarms of particles with similar characteristics, we obtain a result that is essentially identical to the thinned shower, and which is very similar to non-thinned simulations of showers. We call this method dethinning. Using non-thinned showers on a large scale is impossible because of unrealistic CPU time requirements, but with thinned showers that have been dethinned, it is possible to carry out large-scale simulation studies of the detector response for ultra-high energy cosmic ray surface arrays. The dethinning method is described in detail and comparisons are presented with parent thinned showers and with non-thinned showers.

Keywords: cosmic ray, extensive air shower, simulation, thinning

1. Introduction

In the study of ultrahigh energy cosmic rays (UHECR) two main experimental techniques have been used: detection of the fluorescence light emitted by nitrogen molecules excited by the passage of particles in extensive air showers, and detection of the particles themselves when they strike the ground by deploying an array of particle detectors over a large area. Analysis of data from a fluorescence detector involves making a detailed Monte Carlo simulation of the shower, atmosphere, and detector [1] [2]. Only by this technique can the aperture be calculated as a function of energy. Simulation of a large number of complete showers can not be performed using programs like CORSIKA [3] or AIRES [4] because the CPU requirements are too large. The approximation technique called thinning is therefore used, in which particles are removed from consideration in the shower generation and other particles in similar regions of phase space are given weights to account for the loss. Since a fluorescence detector is sensitive to the core region of a shower, where 10^{11} charged particles occur at shower maximum for a 10^{20} eV event, thinning does not harm the accuracy of the simulation. However, for an array of surface detectors (SD), where several km from the core the density of particles is low, the thinning approximation produces an unacceptably coarse simulation of a shower. The average density of particles, as a function of radius from the core, in a thinned shower is approximately correct, but the fluctuations about the average are much larger than in a shower generated without using the thinning approximation. The result of this is that the Monte Carlo technique has been available to those analyzing SD data only in a very limited way.

We have developed a method of performing an accurate Monte Carlo simulation of the surface detector of the Telescope Array (TA) experiment. This method consists of three parts: (1) generating 100 non-thinned CORSIKA showers above $10^{18.5}$ eV using many computer nodes operating in parallel [5], (2) using these showers to develop a method (called dethinning) of replacing much of the shower information lost in thinning, and (3) generating a large number of dethinned showers, including a detailed simulation of the TA surface detector performance, and comparing histograms of important quantities between the data and the Monte Carlo simulation. Reference [5] describes a method for generating CORSIKA showers using many computing nodes in parallel. The present work describes the second step of the method: dethinning. A future paper will describe the third step. This method has proved quite successful, and has allowed us to calculate the aperture of the TA surface detector even in the energy range where its trigger efficiency is not 100%.

The idea of replacing the information lost in thinning was first introduced by P. Billoir [6]. The basic idea in reference [6] and in our work is the same: start with a thinned shower, maintain the average density of particles, and smooth the distribution to get the correct amount of fluctuations. He considered CORSIKA output particles striking the ground in the vicinity of a surface detector (specifically a detector of the Pierre Auger experiment), and, by an oversampling technique based on the CORSIKA output particles, predicted what that detector should observe. He named this technique unthinning. He continued on to estimate several systematic biases to which his method might be sensitive, by studying the properties of thinned and unthinned showers.

Our method, as described in this paper, differs in two ways. First, as the dethinning process we take each CORSIKA output particle with weight w and from it generate a swarm of w

*Corresponding author

Email address: stokes@cosmic.utah.edu (B.T. Stokes)

particles. We perform this step for the entire set of CORSIKA output particles. The details of this generation matter, and are described in this paper. Second, we compare the resulting dethinned showers with showers of almost identical characteristics generated without using the thinning approximation. This is a direct way of testing the accuracy of the dethinning process. Since real surface detectors for ultrahigh energy cosmic rays sample showers coarsely, and measure only the time distribution of the number of particles that strike them, this is the important aspect of the comparison process. We present our comparisons between dethinned showers and non-thinned showers in this manner.

2. Dethinning Description

In a thinned EAS simulation, particles are discarded from the simulation in order to conserve computation time. In the case of CORSIKA [3], for a given thinning level, ε_{th} , if the energy sum of all j secondary particles falls below the thinning energy

$$\varepsilon_{th}E_0 > \sum_j E_j. \quad (1)$$

then only one randomly assigned secondary particle survives with probability

$$p_i = E_i / \sum_j E_j. \quad (2)$$

If the energy sum is greater than the thinning energy, then secondary particles with energy below the thinning energy survive with probability

$$p_i = E_i / (\varepsilon_{th}E_0). \quad (3)$$

In both cases, surviving particles have their weight multiplied by a factor of $w_i = 1/p_i$. Thus the weight of a particle reaching the end of the simulation after passing through k vertices is

$$w_{i,tot} = \prod_k 1/p_k. \quad (4)$$

For sufficiently low values of ε_{th} , it is clear that the thinned simulation output can be thought of as an accurate sample of secondary particle types, trajectories, and positions compared to a non-thinned simulation, for the observable parts of the shower. In this situation, for a particle of weight, w_i , the simulation, on average, removed $w_i - 1$ particles from a similar position in phase space. (Of course, if the value of ε_{th} is increased, this situation is no longer valid because the thinned simulation no longer has the same distribution of particle types, trajectories, and energies as the parent shower.) By comparing a dethinned shower with a similar non-thinned shower one can determine the accuracy of the sampling. The pivotal questions are then: (1) How can a thinned sample be used to reconstruct the full simulation? and (2) What is the maximum value of ε_{th} for which the thinned sample accurately represents the parent shower's particle types, etc.?

We address the first question by describing the process by which we dethin the showers. The original CORSIKA shower

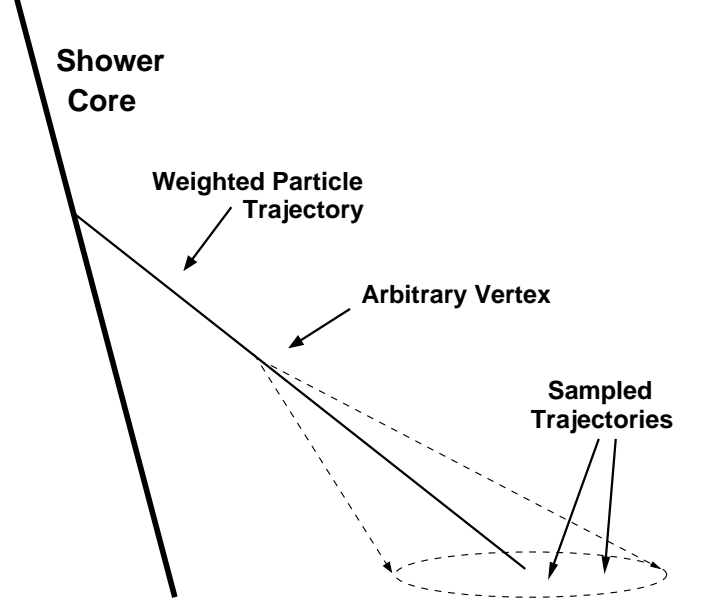


Figure 1: Geometry for a “Gaussian cone” with a vertex placed at arbitrary position on the trajectory of the weighted particle

consists of a list of output particles (plus their weights, types, energies, positions, angles, and arrival time) that have struck the ground. Dethinning consists of adding particles to this list. For every CORSIKA output particle of weight w we add $w - 1$ particles to the list. When this is completed the weight of each particle is set to 1. To insert these particles we use the following procedure (see Figure 1).

1. Choose a vertex point on the trajectory of the weighted particle, in the way given in the next paragraph.
2. Choose a point in a cone centered on the output particle's trajectory, weighted by a two-dimensional Gaussian distribution with a sigma of a few degrees (as described in Section 3). This will be the inserted particle's trajectory.
3. Project the inserted particle to ground level, assign it a time and energy (as described in Section 3), and add it to the particle list of the dethinned shower.
4. Perform steps 2-3 $w - 1$ times. For the case where w is not an integer, add one particle randomly based on the decimal part of w .

There is a maximum distance from the ground that one can choose for the vertex in item 1 above, which is set by the requirement that no particle can have an arrival time that precedes the arrival of the shower front. A too-early arrival time occurs when the total time-of-flight from the point of first interaction, \mathbf{x}_0 , to the vertex point and then to the position on the ground of the generated particle is less than the time-of-flight directly from \mathbf{x}_0 to final particle position. This can be corrected by fixing the position of the vertex point to a position where the time-of-flight from \mathbf{x}_0 to the imaginary vertex and then onward to the final position of the weighted particle, \mathbf{x}_1 is equal to the difference in the arrival time of the weighted particle, t_i , and the time of first interaction, t_0 . This condition is: the distance along the

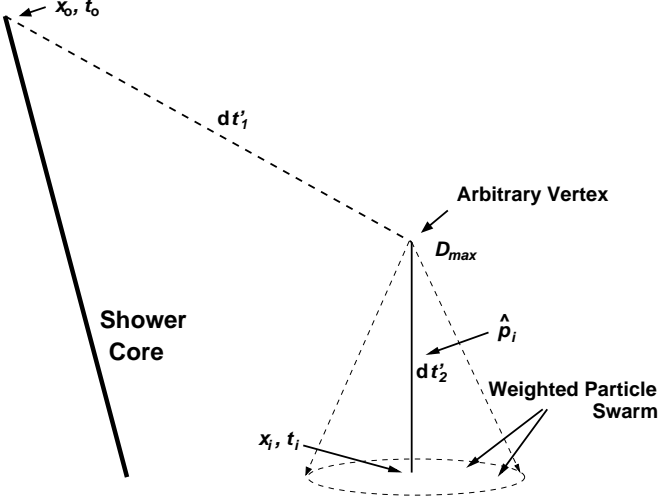


Figure 2: In order to ensure temporal consistency in the EAS simulation, we require $t_i - t_0 \geq dt'_1 + dt'_2$, where t_i is the recorded arrival time for weighted particle and t_0 is the time of first interaction.

weighted particle trajectory, $\hat{\mathbf{p}}_i$, between \mathbf{x}_i and the vertex point is

$$D_{max} = \frac{c^2(t_i - t_0)^2 - |\mathbf{x}_i - \mathbf{x}_0|^2}{2(c(t_i - t_0) - (\mathbf{x}_i - \mathbf{x}_0) \cdot \hat{\mathbf{p}}_i)}, \quad (5)$$

where c is the speed of light. We should emphasize that D_{max} is the maximum separation between the vertex point and the ground. Any shorter separation will also generate dethinned particles that are temporally consistent. The calculation of D_{max} is graphically illustrated in Figure 2.

The second important question pertains to selecting a value of ε_{th} . It should be recalled that in order for this algorithm to work, ε_{th} must be sufficiently small so that the thinned simulation contains a large enough sample of output particles that the distribution of particle types, trajectories, and positions is the same as in the non-thinned simulation. We addressed this question phenomenologically by comparing non-thinned and dethinned showers. Our conclusion was that for $\varepsilon_{th} = 10^{-7}$, this algorithm could be applied without further adjustment. Conversely, for $\varepsilon_{th} = 10^{-5}$, the thinned sample did not contain enough output particles to successfully mimic the properties of a non-thinned shower. The option in between, $\varepsilon_{th} = 10^{-6}$, proved to be a borderline case. We found that dethinning could be successfully implemented by careful adjustment of the available parameters. Because 10^{-6} showers take 1/10 the time to generate as 10^{-7} showers, and require 1/10 as much storage space, $\varepsilon_{th} = 10^{-6}$ proved to be highly desirable so we chose to focus our efforts there.

3. Adjusting the Dethinning Algorithm

In adjusting the dethinning algorithm, we have sought agreement between dethinned and non-thinned simulations for all measures relevant to observation by the TA surface array. These measures include: distributions of secondary particle position and time, particle type, incident angle, and energy.

These measures were tested by comparing thinned versus dethinned versions of the same simulation and then subsequently comparing dethinned simulations versus non-thinned simulations with identical input parameters. Tuning was not considered complete until all measures agreed for lateral distances [500, 4500] m from the shower core.

In the first step, secondary particle spectra for thinned and dethinned versions of the same shower were compared with respect to particle type (photons, electrons, and muons), incident angle with respect to the ground, and position within the shower footprint. The algorithm is tuned so that the particle fluxes after dethinning were consistent with those seen in the original thinned output.

In the second step, distributions of particle fluxes over $6 \times 6 \text{ m}^2$ detector-size areas are compared for dethinned and non-thinned simulations. For this purpose, a library of more than 100 non-thinned showers was generated with parallelized CORSIKA [5]. This library contains showers with $E_0 = [10^{18.5}, 10^{19.5}] \text{ eV}$, $\theta_0 = [0, 60]^\circ$, and proton and iron primary particle types. When identical input parameters are used for thinned and non-thinned simulations, the resulting simulations are not identical. It is therefore necessary to normalize the net secondary particle fluxes of the non-thinned simulation with respect to the thinned simulation. Once this normalization is accomplished the dethinning algorithm can be further refined so that shower particle fluctuations are consistent between dethinned and non-thinned simulations. A further check is done by simultaneously examining dethinned versus non-thinned comparisons over many simulations without normalizing the non-thinned showers. By utilizing the 100 non-thinned showers for this comparison, we ensure that the thinning-dethinning process does not bias the energy scale with respect to non-thinned showers.

The result of adjusting the parameters of the dethinning process is as follows:

1. Angle subtended by Gaussian cone: Set to βd where d is the lateral distance from the shower core for the weighted particle and $\beta = 3^\circ/\text{km}$ for electromagnetic particles and $1^\circ/\text{km}$ for muons and hadrons. The values of β are the minimum necessary to dethin simulations with $\varepsilon_{th} = 10^{-6}$. A smaller value of ε_{th} enables the use of smaller β values.
2. Energy perturbation: Vary the energy of each particle in swarm about a $\pm 10\%$ fractional Gaussian distribution centered on the energy of the original particle. This correction smooths the secondary particle spectra.
3. Minimum lateral distance: Since any detector within a few hundred meters of the shower core is saturated by the large number of particles in that part of a shower, it is not necessary to simulate the central part of a shower; not doing so saves a great deal of CPU time as well. We therefore do not consider in the dethinning process any CORSIKA output particle within a distance r_{min} of the core, and to avoid biases retain only particles farther than r'_{min} from the core. For the case of $\varepsilon_{th} = 10^{-6}$, $r_{min} \geq 100 \text{ m}$, and $r'_{min} - r_{min} \geq 200 \text{ m}$.
4. Particle acceptance: Some particles in the swarm with

longer trajectories than the original weighted particle, if they were followed in the simulation, would not reach the ground. We therefore introduce an acceptance for particles in the swarm with probability: $P = e^{-\Delta\chi/\epsilon}$, where $\Delta\chi$ is the difference in slant depth between the trajectories and $\epsilon = 50 \text{ g/cm}^2$. This is an appreciable correction only for showers with large zenith angle.

5. Height of Gaussian cone: When one sets the vertex a height D_{max} above the ground, this aligns the time at the ground for reintroduced particles, but muons that are created late in the shower then have too wide a spatial distribution. A solution is to set the vertex distance to the smaller of D_{max} and

$$D' = |\mathbf{x}_i - \mathbf{x}_0| - X^{-1}(\mathbf{x}_i, \mathbf{x}_0, \alpha h), \quad (6)$$

where \mathbf{x}_0 is the point of first interaction, h is the generation of the hadron from which the particle originated, $\alpha = 30 \text{ g/cm}^2$, and $X^{-1}(\mathbf{x}_i, \mathbf{x}_0, \alpha h)$ is the distance equivalent of αh slant depth on the trajectory from \mathbf{x}_0 to \mathbf{x}_i .

4. Comparing Simulations: An Example

In Section 3 the method used to tune the dethinning algorithm for $\epsilon_{th} = 10^{-6}$ thinned showers was described. We now consider two examples of comparisons between the dethinned result and the parent thinned shower and with a very similar non-thinned shower. For the comparisons, we use CORSIKA v6.960 [3]. High energy hadronic interactions are modeled by QGSJET-II-03 [7], low energy hadronic interactions are modeled by FLUKA2008.3c [8][9], and electromagnetic interactions are modeled by EGS4 [10]. For the thinned shower, $\epsilon = 10^{-6}$ and additionally, we apply the thinning optimization scheme proposed by Kobal [11].

For both comparisons, the shower footprint is divided into eight 500 m thick ring-shaped segments from 500 to 4500 m in lateral distance. Each lateral ring is further divided into six pie-shaped wedges with respect to the rotation angle about the shower axis.

For the first comparison, we divide the particle flux into ten $\cos \theta_i = 0.1$ bins, where θ_i is the incident angle of an individual particle with respect to the ground. Three particle types are considered: photons, electrons, and muons (all other types are relatively scarce). Each bin is then histogrammed with respect to energy. This results in $8 \times 6 \times 10 \times 3 = 1440$ discrete secondary particle energy spectra. By scanning through these spectra, any discrepancies in particle flux generated by dethinning can be readily identified. Figures 3 and 4 show examples, typical of all 1440 spectra, of these comparisons. The agreement is excellent, showing that the process of smoothing the distribution of particles does not change the angular or energy distribution of particles from the parent thinned shower.

Having established that dethinning maintains the large-scale secondary particle fluxes from parent thinned simulations, we then turn to comparisons with non-thinned showers produced with a parallelized version of CORSIKA [5]. Because it is structurally impossible in CORSIKA to produce identical thinned and non-thinned simulations, for this comparison it is

necessary to normalize the net particle flux of the non-thinned and thinned (not dethinned) simulations. This is done separately for each wedge-shaped region of the shower footprint and each particle type.

For the comparison, we consider the same segments in the shower footprint as for Figures 3 and 4. The segment is then further divided into $6 \times 6 \text{ m}^2$ tiles covering the distances from 500 m to 4500 m from the core. These tiles are then projected onto the ground, and for each tile we tabulate the time, $t_{1/10}$, when 10% of the total particle flux has arrived, the time, $t_{1/2}$, when 50% of the total particle flux has arrived, and the flux of all photons, electrons, and muons. The times are then corrected for the time offset between the positions of each segment on the ground and in the plane normal to the EAS. Figures 5 through 9 show the results of this comparison. They show that for the dethinned shower the time of arrival and number of particles per tile agree very well with that of the non-thinned shower.

5. Conclusion

The aim of this dethinning method is to use a thinned simulation to reconstruct, on a statistical basis, information lost in the thinning process. Since thinning preserves mean particle densities as a function of radius from the shower core, but introduces large biases into the distribution of the densities (e.g., the RMS of the particle distribution), dethinning is designed to be a smoothing procedure. The dethinning process is tuned to maintain mean particle densities from parent thinned showers, and reproduces distributions of arrival times and numbers of particles striking counter-size areas in non-thinned showers. Since these are the distributions to which surface detectors of experiments are sensitive, dethinned showers can be used in place of non-thinned showers in comparisons with data.

This method has three primary limitations. We require that $\epsilon_{th} \leq 10^{-6}$ and lateral distances be restricted to less than 4500 m from the shower core. Beyond these limits we cannot reliably control for artificial fluctuations. We have tested this process for $\theta_0 < 60^\circ$ but have not yet examined the case of more inclined showers.

We have compared dethinned shower simulations against both thinned and non-thinned simulations, and shown that the dethinning process reproduces the characteristics of CORSIKA/QGSJET-II-03 showers generated without thinning. In a future paper in this series we will show that the resulting showers reproduce the characteristics of the TA surface array data.

Dethinning is proving to be a powerful tool for studying and understanding UHECR observations by enabling a thorough simulation of surface array data. This enables a direct comparison between Monte Carlo simulations and TA surface array data and results in a more complete understanding of the response of the detector. This understanding leads to the ability to accurately assess detector aperture for efficiencies far less than 100%, which in turn leads to significant improvements in the measurement of the cosmic ray spectrum, and in the estimation of the detector exposure to the sky for astronomical studies.

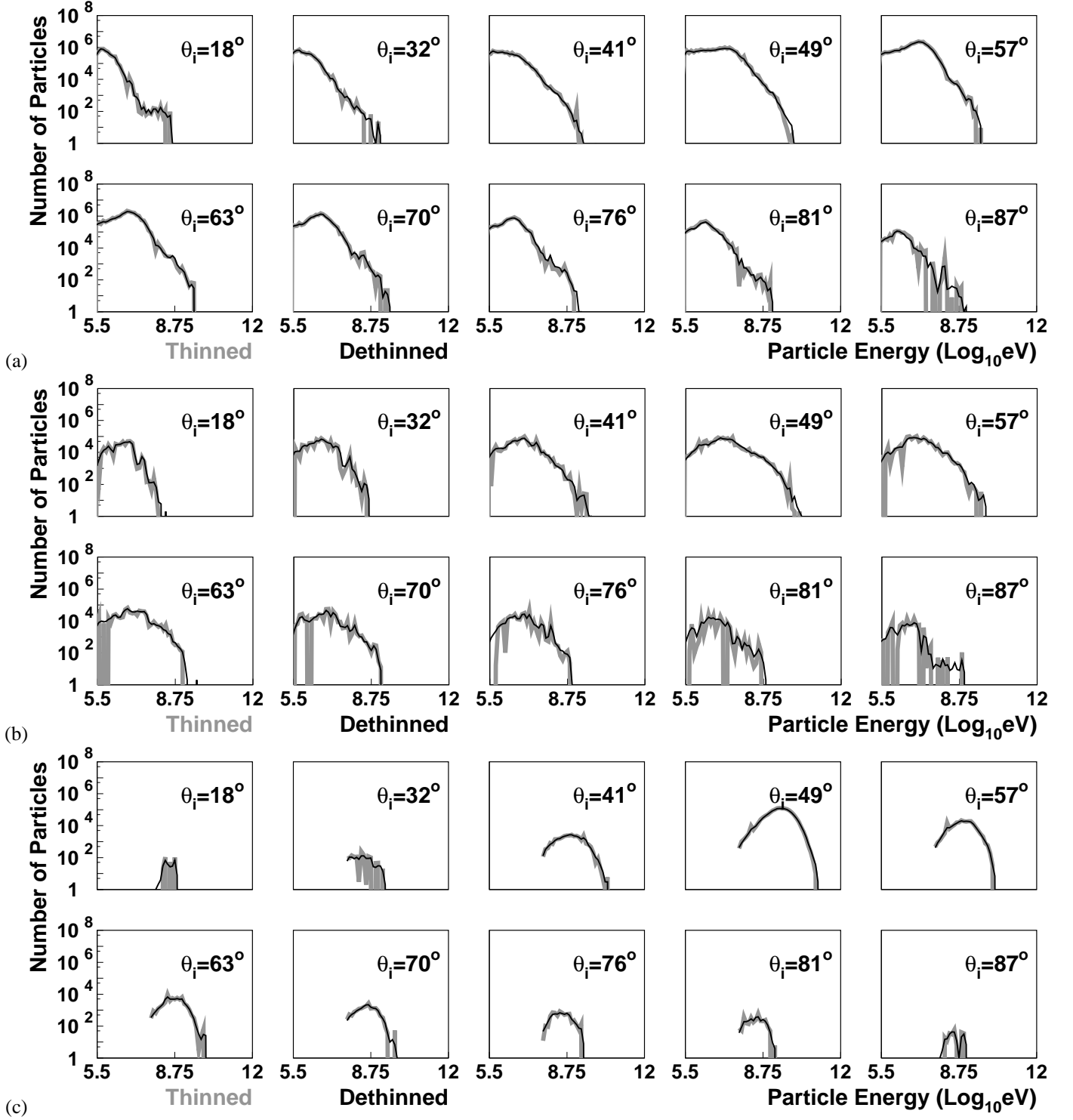


Figure 3: Comparison of secondary particle spectra with and without dethinning for a thinned simulation of a protonic EAS with primary energy $E_0 = 10^{19.0}$ eV and primary zenith angle $\theta_0 = 45^\circ$. In both cases, the secondary particles whose ground position was within a region enclosed by shower rotation angles, $\Phi = [-30^\circ, 30^\circ]$ (with respect to the primary azimuthal direction) and lateral distances, $r = [500\text{m}, 1000\text{m}]$ were tabulated according to particle type, incident angle with respect to the ground, θ_i , and kinetic energy. In the case of the thinned simulation, each secondary particle with weight, w_i , was treated as w_i identical particles. The resulting spectral comparisons are shown in $\cos \theta_i = 0.1$ increment bins for a) photons, b) electrons, and c) muons. For each histogram, good agreement is observed between thinned simulations (gray) and dethinned (black).

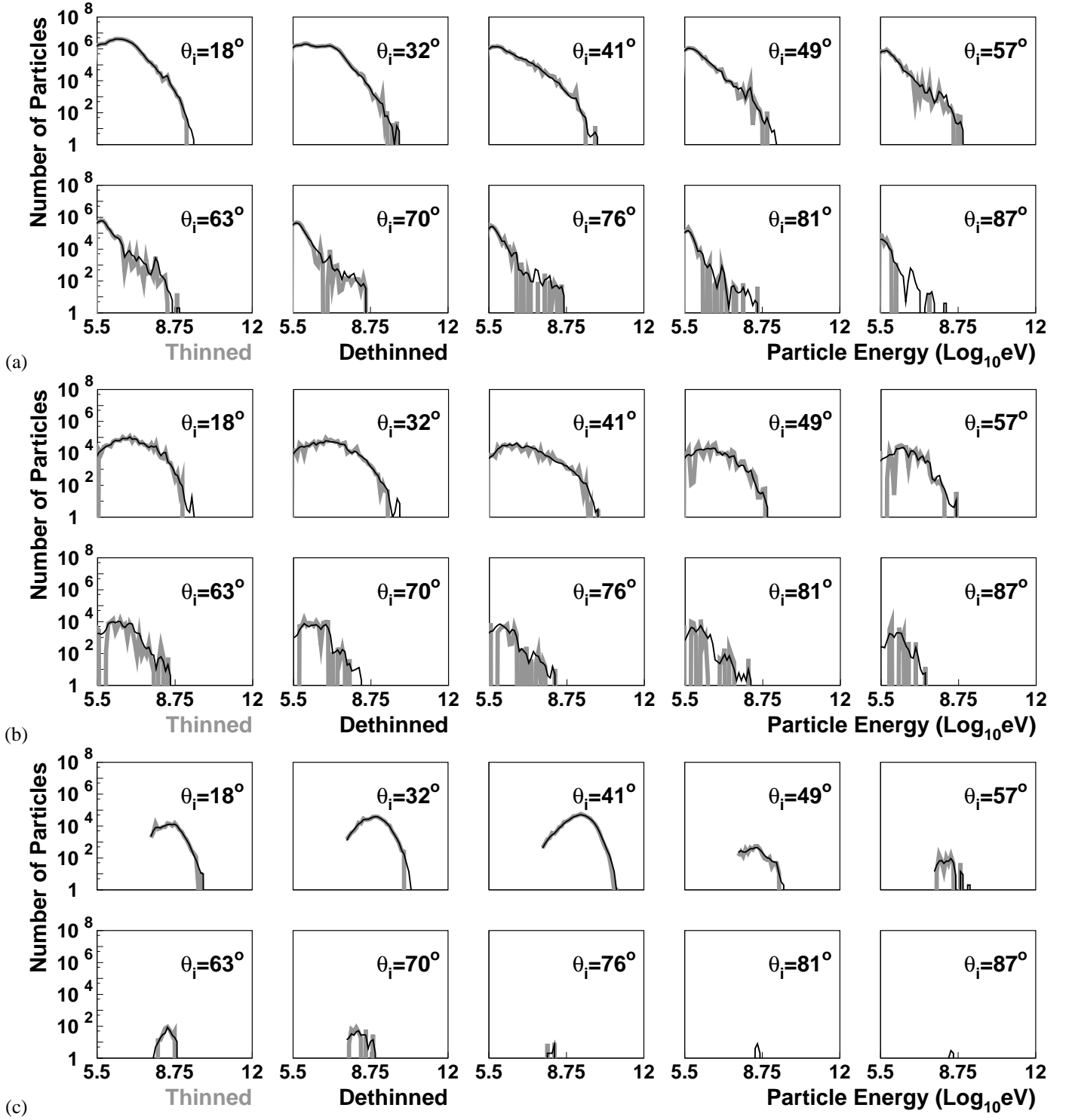


Figure 4: Comparison of secondary particle spectra with and without dethinning for a thinned simulation of a protonic EAS with primary energy $E_0 = 10^{19.0}$ eV and primary zenith angle $\theta_0 = 45^\circ$. In both cases, the secondary particles whose ground position was within a region enclosed by shower rotation angles, $\Phi = [150^\circ, 210^\circ]$ (with respect to the primary azimuthal direction) and lateral distances, $r = [1500\text{m}, 2000\text{m}]$ were tabulated according to particle type, incident angle with respect to the ground, θ_i , and kinetic energy. In the case of the thinned simulation, each secondary particle with weight, w_i , was treated as w_i identical particles. The resulting spectral comparisons are shown in $\cos \theta_i = 0.1$ increment bins for a) photons, b) electrons, and c) muons. For each histogram, good agreement is observed between thinned simulations (gray) and dethinned (black).

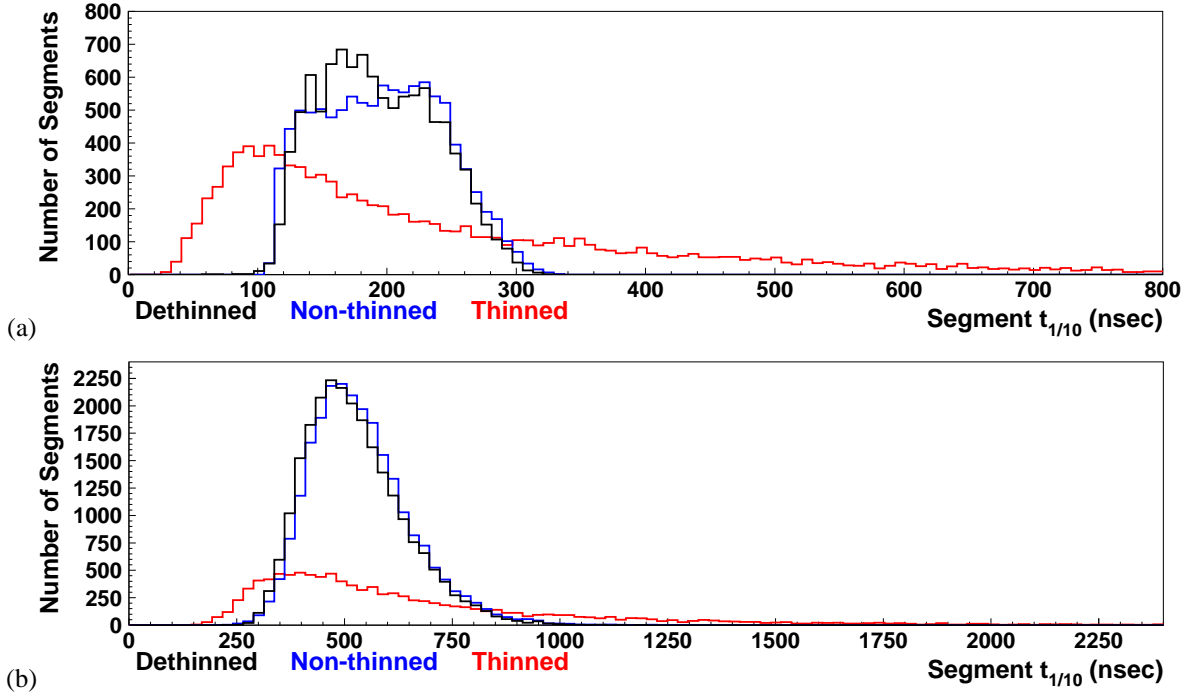


Figure 5: Comparison of the distribution of rise times, $t_{1/10}$, where 10% of the total particle flux has arrived for a given $6 \times 6 \text{ m}^2$ segment in plane normal to shower trajectory for $10^{19.0} \text{ eV}$ protonic EAS simulations with a primary zenith angle of 45° . For this comparison, $t_{1/10}$ was measured for segments within a) a region enclosed by shower rotation angles, $\Phi = [-30^\circ, 30^\circ]$ (with respect to the primary azimuthal direction) and lateral distances, $r = [500\text{m}, 1000\text{m}]$ and b) a region enclosed by shower rotation angles, $\Phi = [150^\circ, 210^\circ]$ (with respect to the primary azimuthal direction) and lateral distances, $r = [1500\text{m}, 2000\text{m}]$. In both cases, the distribution of $t_{1/10}$ values is consistent for the dethinned (black) and non-thinned (blue) simulations while the thinned (red) simulation is quite different.

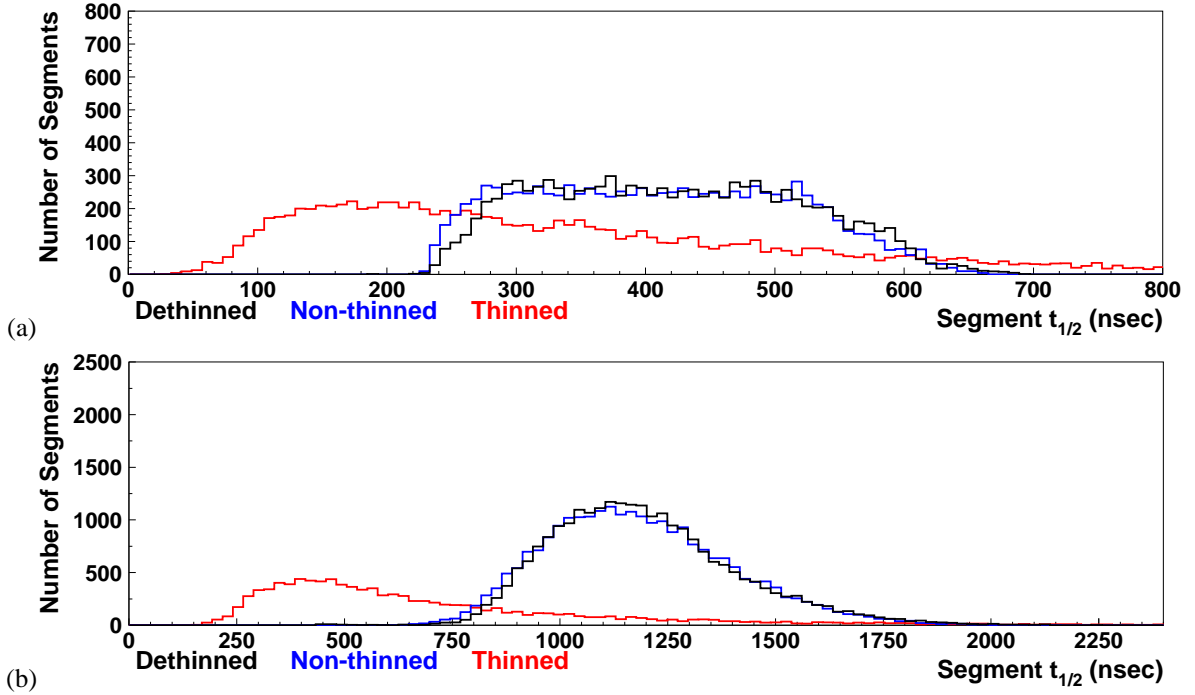


Figure 6: Comparison of the distribution of median arrival times, $t_{1/2}$, where 50% of the total particle flux has arrived for a given $6 \times 6 \text{ m}^2$ segment in plane normal to shower trajectory for $10^{19.0} \text{ eV}$ protonic EAS simulations with a primary zenith angle of 45° . For this comparison, $t_{1/2}$ was measured for segments within a) a region enclosed by shower rotation angles, $\Phi = [-30^\circ, 30^\circ]$ (with respect to the primary azimuthal direction) and lateral distances, $r = [500\text{m}, 1000\text{m}]$ and b) a region enclosed by shower rotation angles, $\Phi = [150^\circ, 210^\circ]$ (with respect to the primary azimuthal direction) and lateral distances, $r = [1500\text{m}, 2000\text{m}]$. In both cases, the distribution of $t_{1/2}$ values is consistent for the dethinned (black) and non-thinned (blue) simulations while the thinned (red) simulation is quite different.

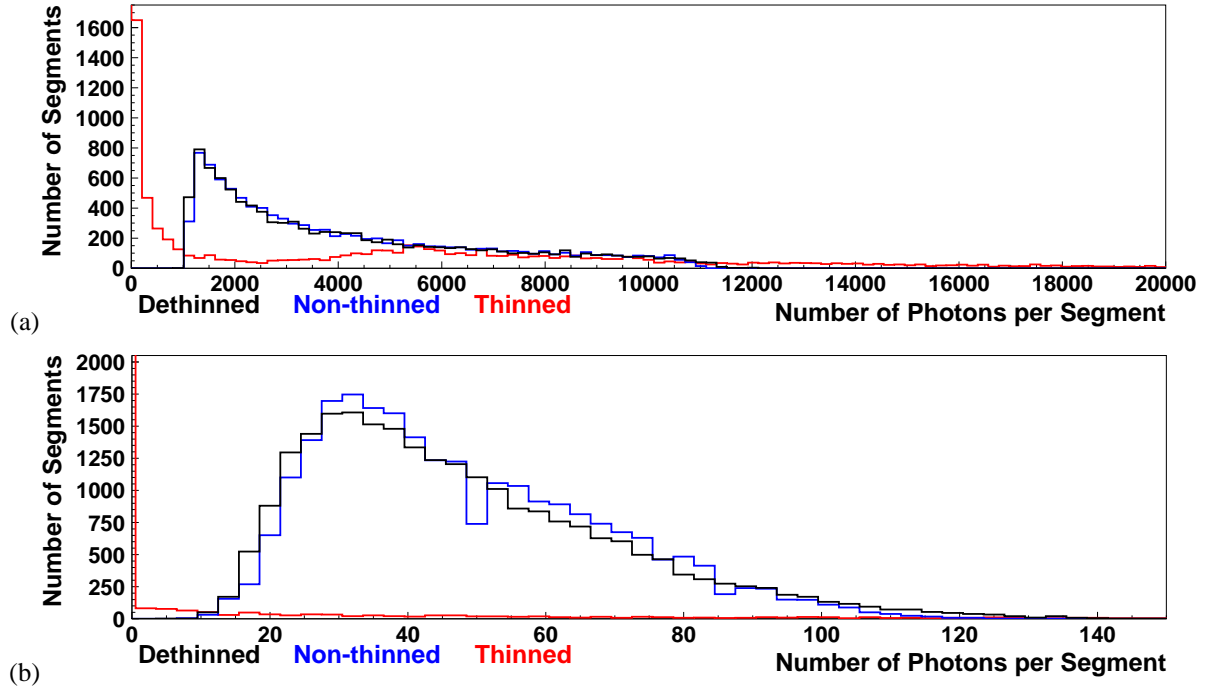


Figure 7: Comparison of the distribution of photon flux measurements for $6 \times 6 \text{ m}^2$ segments in plane normal to shower trajectory for $10^{19.0} \text{ eV}$ protonic EAS simulations with a primary zenith angle of 45° . For this comparison, photon flux measurements were done for segments within a) a region enclosed by shower rotation angles, $\Phi = [-30^\circ, 30^\circ]$ (with respect to the primary azimuthal direction) and lateral distances, $r = [500\text{m}, 1000\text{m}]$ and b) a region enclosed by shower rotation angles, $\Phi = [150^\circ, 210^\circ]$ (with respect to the primary azimuthal direction) and lateral distances, $r = [1500\text{m}, 2000\text{m}]$. In both cases, the distribution of photon flux values is consistent for the dethinned (black) and non-thinned (blue) simulations while the thinned (red) simulation is quite different.

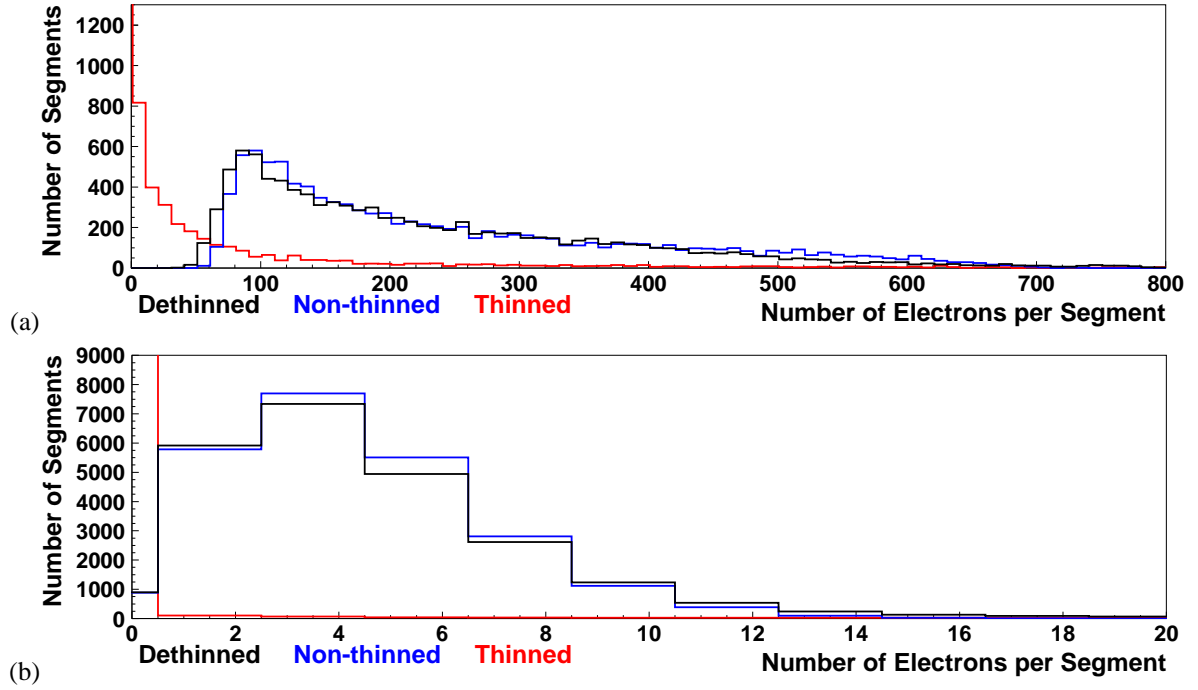


Figure 8: Comparison of the distribution of electron flux measurements for $6 \times 6 \text{ m}^2$ segments in plane normal to shower trajectory for $10^{19.0} \text{ eV}$ protonic EAS simulations with a primary zenith angle of 45° . For this comparison, electron flux measurements were done for segments within a) a region enclosed by shower rotation angles, $\Phi = [-30^\circ, 30^\circ]$ (with respect to the primary azimuthal direction) and lateral distances, $r = [500\text{m}, 1000\text{m}]$ and b) a region enclosed by shower rotation angles, $\Phi = [150^\circ, 210^\circ]$ (with respect to the primary azimuthal direction) and lateral distances, $r = [1500\text{m}, 2000\text{m}]$. In both cases, the distribution of electron flux values is consistent for the dethinned (black) and non-thinned (blue) simulations while the thinned (red) simulation is quite different.

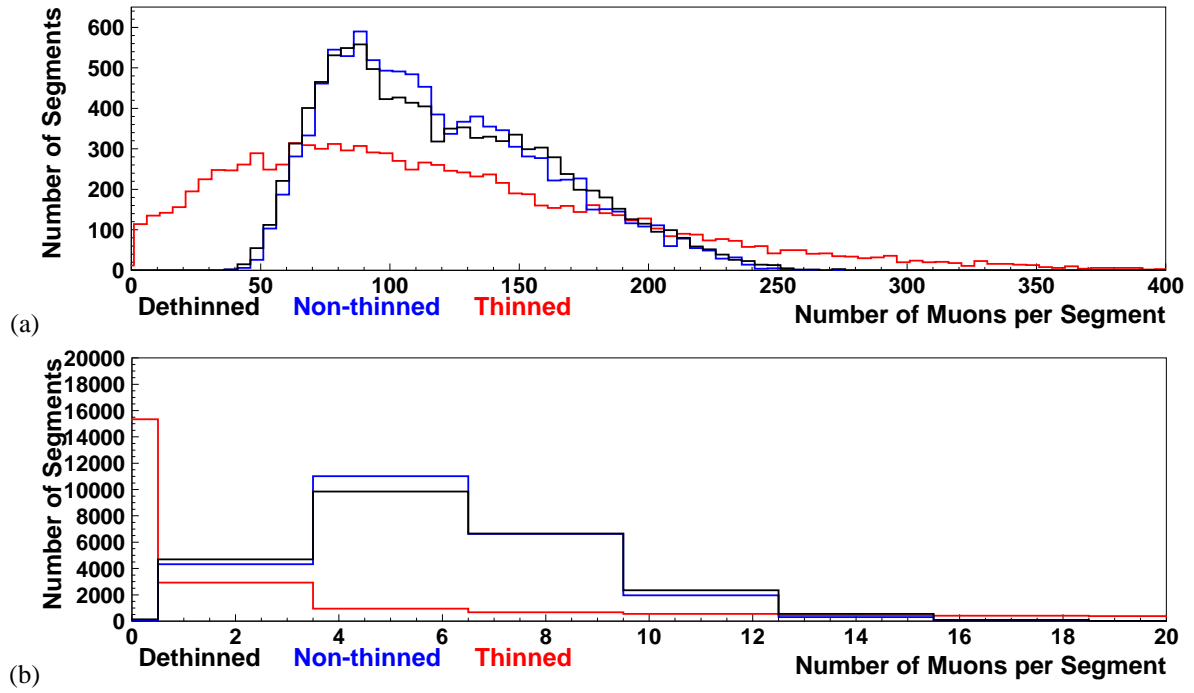


Figure 9: Comparison of the distribution of muon flux measurements for $6 \times 6 \text{ m}^2$ segments in plane normal to shower trajectory for $10^{19.0} \text{ eV}$ protonic EAS simulations with a primary zenith angle of 45° . For this comparison, muon flux measurements were done for segments within a) a region enclosed by shower rotation angles, $\Phi = [-30^\circ, 30^\circ]$ (with respect to the primary azimuthal direction) and lateral distances, $r = [500\text{m}, 1000\text{m}]$ and b) a region enclosed by shower rotation angles, $\Phi = [150^\circ, 210^\circ]$ (with respect to the primary azimuthal direction) and lateral distances, $r = [1500\text{m}, 2000\text{m}]$. In both cases, the distribution of muon flux values is consistent for the dethinned (black) and non-thinned (blue) simulations while the thinned (red) simulation is quite different.

6. Acknowledgments

This work was supported by the U.S. National Science Foundation awards PHY-0601915, PHY-0703893, PHY-0758342, and PHY-0848320 (Utah) and PHY-0649681 (Rutgers). The simulations presented herein have only been possible due to the availability of computational resources at the Center for High Performance Computing at the University of Utah which is gratefully acknowledged. A portion of the computational resources for this project has been provided by the U.S. National Institutes of Health (Grant # NCRR 1 S10 RR17214-01) on the Arches Metacluster, administered by the University of Utah Center for High Performance Computing.

References

- [1] R. U. . Abbasi, et al., Monocular measurement of the spectrum of UHE cosmic rays by the FADC detector of the HiRes experiment, *Astropart. Phys.* 23 (2005) 157–174. [arXiv:astro-ph/0208301](#), [doi:10.1016/j.astropartphys.2004.12.006](#).
- [2] L. Perrone, Measurement of the UHECR energy spectrum from hybrid data of the Pierre Auger Observatory, in: *Proceedings of the 30th ICRC*, Vol. 4, Merida, 2007, pp. 331–334. [arXiv:0706.2643](#).
- [3] D. Heck, G. Schatz, T. Thouw, J. Knapp, J. N. Capdevielle, CORSIKA: A Monte Carlo code to simulate extensive air showers, *Tech. Rep.* 6019, FZKA (1998).
- [4] S. J. Sciutto, AIRES: A system for air shower simulations, *Tech. Rep.* 2.6.0, UNLP (2002).
- [5] B. T. Stokes, et al., A simple parallelization scheme for extensive air shower simulations, submitted to *Astroparticle Physics* (2011). [arXiv:1103.4643](#).
- [6] P. Billoir, A sampling procedure to regenerate particles in a ground detector from a “thinned” air shower simulation output, *Astropart. Phys.* 30 (2008) 270–285. [doi:10.1016/j.astropartphys.2008.10.002](#).
- [7] S. Ostapchenko, QGSJET-II: Towards reliable description of very high energy hadronic interactions, *Nucl. Phys. Proc. Suppl.* 151 (2006) 143–146. [arXiv:hep-ph/0412332](#), [doi:10.1016/j.nuclphysbps.2005.07.026](#).
- [8] A. Ferrari, P. R. Sala, A. Fasso, J. Ranft, FLUKA: A multi-particle transport code (Program version 2005), *Tech. Rep.* 2005-010, CERN (2005).
- [9] G. Battistoni, et al., The FLUKA code: Description and benchmarking, *AIP Conf. Proc.* 896 (2007) 31–49. [doi:10.1063/1.2720455](#).
- [10] W. R. Nelson, H. Hirayama, D. W. O. Rogers, The EGS4 code system, *Tech. Rep.* 0265, SLAC (1985).
- [11] M. Kobal, A thinning method using weight limitation for air-shower simulations, *Astropart. Phys.* 15 (2001) 259–273. [doi:10.1016/S0927-6505\(00\)00158-4](#).